June 7, 2008

# Manipulating microparticles with single surface-immobilized nanoparticles

J Zhang
S Srivastava
R Duffadar
JM Davis
VM Rotello, et al.

# Manipulating Microparticles with Single Surface-Immobilized Nanoparticles

Jun Zhang,[†] Sudhanshu Srivastava,[‡] Ranojoy Duffadar,[§] Jeffrey M. Davis,[§] Vincent M. Rotello,[‡] and Maria M. Santore*,[†]

*Department of Polymer Science and Engineering, Department of Chemistry, and Department of Chemical Engineering, University of Massachusetts, Amherst, Massachusetts 01003*

*Received March 18, 2008. Revised Manuscript Received May 6, 2008*

This experimental study explores the capture and manipulation of micrometer-scale particles by single surface-immobilized nanoparticles. The nanoparticles, approximately 10 nm in diameter, are cationic and therefore attract the micrometer-scale silica particles in an analyte suspension. The supporting surface on which the nanoparticles reside is negative (also silica) and repulsive toward approaching microparticles. In the limit where there are as few as 9 nanoparticles per square micrometer of collector, it becomes possible to capture and hold micrometer-scale silica particles with single nanoparticles. The strong nanoparticle−microparticle attractions, their nanometer-scale protrusion forward of the supporting surface, and their controlled density on the supporting surface facilitate microparticle−surface contact occurring through a single nanoelement. This behavior differs from most particle−particle, cell−cell, or particle (or cell)−surface interactions that involve multiple ligand−receptor bonds or much larger contact areas. Despite the limited contact of microparticles with surface-immobilized nanparticles, microparticles resist shear forces of 9 pN or more but can be released through an increase in the ionic strength. The ability of nanoparticles to reversibly trap and hold much larger targets has implications in materials self-assembly, cell capture, and sorting applications, whereas the single point of contact affords precision in particle manipulation.

## Introduction

Dynamic particle capture and adhesion have long been recognized to be important in technological applications ranging from aerosol handling to tribology. This significance now extends into the biological arena. For instance, flowing cells and bacteria are captured on surfaces when neutrophils roll on an injury-activated endothelium, during cancer metastasis, and upon initiation of viral and bacterial infection. These behaviors have been reproduced ex vivo with both cells[1–3] and rigid round particles functionalized with adhesion proteins[4] to demonstrate the underlying principles. Sophisticated biomaterials that achieve similar dynamic and selective control of cells are, therefore, logical candidates for the next generation of diagnostic devices and systems for the refinement of cell suspensions for tissue engineering.

Currently, most research on cell−biomaterial adhesion focuses on the development of materials that bind cells via relatively dense receptor placement on a surface[5–8] (or tethered from the surface[8–11]) or relatively concentrated distributions of receptor-bearing nanoparticles.[12–14] Under quiescent conditions, there is an optimal receptor loading for cell proliferation or differentiation:[10,15,16] multiple contacts between the cell and receptors on biomaterials stimulate the formation of an oriented actin network within each cell.[5] Likewise, multiple interaction sites between cells comprise the mechanism for infection,[17] immune response,[18–20] fertilization,[21] and differentiation[22] of cells. Indeed, Nature seems to have good reason to rely on many weak interactions rather than a few strong ones for cell adhesion and signaling.[21,23] At the opposite extreme, however, there is technological value to biomaterial−cell interactions generated by one or a few strong contacts. With reports of a receptor threshold for communication between cells,[19,20,24,25] materials that capture cells with a limited number of contacts may be able

* Corresponding author. Tel: 413-577-1417. Fax: 413-545-0082. E-mail: santore@mail.pse.umass.edu.
[†] Department of Polymer Science and Engineering.
[‡] Department of Chemistry.
[§] Department of Chemical Engineering.

(1) Lawrence, M. B.; Springer, T. A. *Cell* **1991**, *65*, 859–873.
(2) Thomas, W. E.; Nilsson, L. M.; Forero, M.; Sokurenko, E. V.; Vogel, V. *Mol. Microbiol.* **2004**, *53*, 1545–1557.
(3) Pauli, B. U.; Augustinvoss, H. G.; Elsabban, M. E.; Johnson, R. C.; Hammer, D. A. *Cancer Metastasis Rev.* **1990**, *9*, 175–189.
(4) Brunk, D. K.; Goetz, D. J.; Hammer, D. A. *Biophys. J.* **1996**, *71*, 2902–2907.
(5) Massia, S. P.; Hubbell, J. A. *J. Cell Biol.* **1991**, *114*, 1089–1100.
(6) Rezania, A.; Healy, K. E. *Biotechnol. Prog.* **1999**, *15*, 19–32.
(7) Felsenfeld, D. P.; Choquet, D.; Sheetz, M. P. *Nature* **1996**, *383*, 438–440.
(8) Hern, D. L.; Hubbell, J. A. *J. Biomed. Mater. Res.* **1998**, *39*, 266–276.
(9) Shu, X. Z.; Ghosh, K.; Liu, Y. C.; Palumbo, F. S.; Luo, Y.; Clark, R. A.; Prestwich, G. D. *J. Biomed. Mater. Res., Part A* **2004**, *68A*, 365–375.
(10) Neff, J. A.; Tresco, P. A.; Caldwell, K. D. *Biomaterials* **1999**, *20*, 2377–2393.
(11) Schmidt, D. R.; Kao, W. J. *J. Biomed. Mater. Res., Part A* **2007**, *83A*, 617–625.
(12) Montet, X.; Funovics, M.; Montet-Abou, K.; Weissleder, R.; Josephson, L. *J. Med. Chem.* **2006**, *49*, 6087–6093.
(13) Selhuber, C.; Blummel, J.; Czerwinski, F.; Spatz, J. P. *Nano Lett.* **2006**, *6*, 267–270.
(14) Graeter, S. V.; Huang, J. H.; Perschmann, N.; Lopez-Garcia, M.; Kessler, H.; Ding, J. D.; Spatz, J. P. *Nano Lett.* **2007**, *7*, 1413–1418.
(15) Maheshwari, G.; Brown, G.; Lauffenburger, D. A.; Wells, A.; Griffith, L. G. *J. Cell Sci.* **2000**, *113*, 1677–1686.
(16) Rowley, J. A.; Mooney, D. J. *J. Biomed. Mater. Res.* **2002**, *60*, 217–223.
(17) Platt, E. J.; Wehrly, K.; Kuhmann, S. E.; Chesebro, B.; Kabat, D. *J. Virol.* **1998**, *72*, 2855–2864.
(18) Freeman, G. J.; Long, A. J.; Iwai, Y.; Bourque, K.; Chernova, T.; Nishimura, H.; Fitz, L. J.; Malenkovich, N.; Okazaki, T.; Byrne, M. C.; Horton, H. F.; Fouser, L.; Carter, L.; Ling, V.; Bowman, M. R.; Carreno, B. M.; Collins, M.; Wood, C. R.; Honjo, T. *J. Exp. Med.* **2000**, *192*, 1027–1034.
(19) Viola, A.; Lanzavecchia, A. *Science* **1996**, *273*, 104–106.
(20) Carter, R. H.; Fearon, D. T. *Science* **1992**, *256*, 105–107.
(21) Mann, D. A.; Kanai, M.; Maly, D. J.; Kiessling, L. L. *J. Am. Chem. Soc.* **1998**, *120*, 10575–10582.
(22) Robertson, K. A.; Emami, B.; Mueller, L.; Collins, S. J. *Mol. Cell. Biol.* **1992**, *12*, 3743–3749.
(23) Arnaud, C. H. *Chem. Eng. News* **2007**, *85* (8), 10.
(24) Moro, L.; Venturino, M.; Bozzo, C.; Silengo, L.; Altruda, F.; Beguinot, L.; Tarone, G.; Defilippi, P. *EMBO J.* **1998**, *17*, 6622–6632.
(25) Sarda, S.; Pointu, D.; Pincet, F.; Henry, N. *Biophys. J.* **2004**, *86*, 3291–3303.

10.1021/la800857v CCC: $40.75 
Published on Web 06/07/2008

to do so without the cell's knowledge. That is, limiting the numbers of contacts may facilitate cell manipulation without signaling. Likewise, surfaces that trap cells and particles with just a few or even a single contact can also provide highly sensitive detecting and sensing elements.

The goal of capturing cells and other micrometer-scale objects with minimal interactions motivates the current study, which develops a cell-free and biomolecule-free system to explore how localized (~10 nm, the size of proteins) attractive surface regions can capture and adhere much larger flowing micrometer-scale particles, even though the background surface and hydrodynamic fields are substantially repulsive. This nonbiological approach quantitatively demonstrates, without commitment to a particular ligand−receptor pair, the physics important to particle adhesion in the limit of one binding site per microparticle. Our surface design strategy recreates the most important features of the cell surface: on cells, attractions occur at distinct points (receptors) whereas the glycocalyx provides a background field that is repulsive to most biological objects. The current study employs a parallel construction: an electrostatically repulsive background field in which attractive nanoparticle-based adhesive elements are distributed. The work identifies a regime where micrometer-scale objects, representative of bacteria and biological cells, are captured and held by single-nanoparticle surface constructs.

This study, employing cationic nanoparticles as adhesive elements, distinguishes itself from our prior work that probes particle capture with flat cationic patches.[26–28] Qualitative differences between the adhesive behavior in the nanoparticle system and that using patches are demonstrated. Furthermore, with the adherent nanoparticles, we examine the strength of binding by attempting to dislodge adherent microparticles with flow, in the limit where the microparticles are held by a single nanoparticle. We demonstrate that the electrostatic attractions, even for a single 10 nm contact region, can be tuned to be far in excess of accessible hydrodynamic forces, or they can be tuned to be small relative to hydrodynamic forces. The nanoparticle-containing surfaces therefore exhibit highly efficient capture and a tunable means of particle and cell manipulation: future application of these design principles will facilitate the creation of extremely sensitive detecting surfaces and surfaces that capture, adhere, and release cells, with minimal biological response. The findings here are also relevant to technologies exploiting mixed flocculation conditions, following advances in heteroflocculation.[29–37] Indeed, much research has focused on the ionic conditions surrounding the aggregation of large particles by smaller ones of opposite charge. The current work is related in that the normalization of adhesion rate plots on the transport-limited maximum converts to the inverse of the well-known "stability factor."

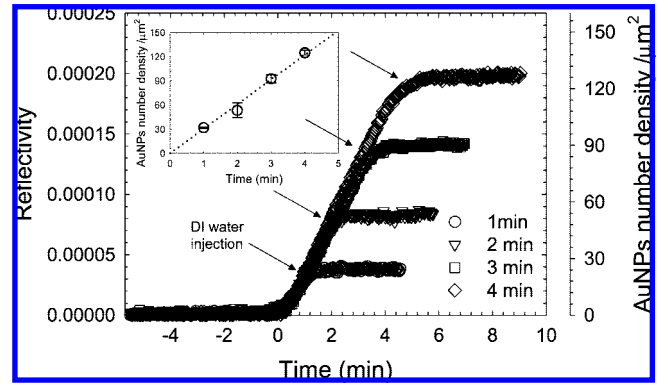


**Figure 1.** Representative data for the deposition of cationic gold nanoparticles on acid-etched microscope slides as measured by near-Brewster reflectometry. The nanoparticle concentration is 20 ppm in DI water with a shear rate of 10 $s^{-1}$. Arrows indicate the reinjection of DI water to stop additional particle deposition. Cationic nanoparticles were then retained in flowing DI water, as indicated by the flat signal after the reinjection of DI water. The inset shows average deposition amounts for several runs of different deposition times.

## Experimental Description

Our system consists of a negative surface (silica) that electrostatically repels negative objects (monodisperse silica microparticles) but contains 11 nm nanoparticles that are densely positively charged. The cationic nanoparticles were built from 7.5 nm gold cores with a shell of approximately 500 ligands: 200 *N*,*N*,*N*-trimethyl(11-mercaptoundecyl)ammonium chloride side chains and 300 1-mercaptoundecane chains. This brought the diameter of the nanoparticles up to 11 nm (dry, by TEM) or 15 nm in solution as measured by dynamic light scattering.[38] Each nanoparticle therefore contained 200 quaternary amines distributed over its otherwise hydrophobic surface ($4\pi r^2 = 380$ nm$^2$) with an average spacing of 1.38 nm. The zeta potentials of these nanoparticles were 20.5 ± 3.3 mV in DI water and 26.6 ± 1.3 in 5 mM pH 6.1 phosphate buffer.

To create collecting surfaces, cationic nanoparticles were randomly deposited from dilute aqueous solution (20 ppm in DI water) on the silica surfaces of acid-etched microscope slides[39] using a slit shear flow cell with a known mass transport coefficient.[39,40] The nanoparticle density could therefore be precisely controlled through the flow time of the nanoparticle suspension.[41] After the desired flow time, DI water was reinjected into the chamber to halt nanoparticle deposition. Figure 1 presents examples of the nanoparticle deposition curves, measured by near-Brewster optical reflectometry,[39] with the AFM images of the resulting surfaces in Figure 2, obtained after the surfaces were rinsed and dried. (The flow rate for this particular series was 10 $s^{-1}$.) The bound nanoparticle density is linear in flow time over the range of interest, below saturation of the surface by gold nanoparticles. The deposition rate (30 particles/$\mu$m$^2$ min in this example) is generally proportional to the nanoparticle concentration in solution and scales as the flow rate to the $^1/_3$ power, as expected for mass-transport particle deposition.[42] Indeed, the number of particles per unit area, as measured by AFM, quantitatively agrees with the mass-transport-limited nanoparticle deposition rates from Brewster reflectometry (for particles with a 15 nm hydrodynamic radius), providing confidence that the particle densities (number of nanoparticles per area) in Figure 2 are representative of much larger surface areas on the order of millimeters, as seen by reflectometry. The ultimate arrangement of the particles on the surface is random and tends not to contain closely positioned nanoparticles. These observations are consistent with strong nano-

(26) Santore, M. M.; Kozlova, N. *Langmuir* **2007**, *23*, 4782–4791.
(27) Kozlova, N.; Santore, M. M. *Langmuir* **2006**, *22*, 1135–1142.
(28) Kalasin, S.; Santore, M. M. *Langmuir* **2008**, *24*, 4435–4438.
(29) Asselman, T.; Garnier, G. *Langmuir* **2000**, *16*, 4871–4876.
(30) Harley, S.; Thompson, D. W.; Vincent, B. *Colloids Surf.* **1992**, *62*, 163–176.
(31) Islam, A. M.; Chowdhry, B. Z.; Snowden, M. J. *Adv. Colloid Interface Sci.* **1995**, *62*, 109–136.
(32) Kim, A. Y.; Hauch, K. D.; Berg, J. C.; Martin, J. E.; Anderson, R. A. *J. Colloid Interface Sci.* **2003**, *260*, 149–159.
(33) Luckham, P. F.; Vincent, B.; Tadros, T. F. *Colloids Surf.* **1983**, *6*, 119–133.
(34) Porubska, J.; Alince, B.; van de Ven, T. G. M. *Colloids Surf., A* **2002**, *210*, 223–230.
(35) Puertas, A. M.; Fernandez-Barbero, A.; de las Nieves, F. J. *J. Chem. Phys.* **2001**, *115*, 5662–5668.
(36) vandeVen, T. G. M.; Alince, B. *J. Colloid Interface Sci.* **1996**, *181*, 73–78.
(37) Wall, S.; Samuelsson, P.; Degerman, G.; Skoglund, P.; Samuelsson, A. *J. Colloid Interface Sci.* **1992**, *151*, 178–188.
(38) Srivastava, S.; Samanta, B.; Jordan, B. J.; Hong, R.; Xiao, Q.; Tuominen, M. T.; Rotello, V. M. *J. Am. Chem. Soc.* **2007**, *129*, 11776–11780.
(39) Fu, Z. G.; Santore, M. M. *Colloids Surf., A* **1998**, *135*, 63–75.
(40) Shibata, C. T.; Lenhoff, A. M. *J. Colloid Interface Sci.* **1992**, *148*, 485–507.
(41) Toscano, A.; Santore, M. M. *Langmuir* **2006**, *22*, 2588–2597.
(42) Leveque, M. A. *Ann. Mines* **1928**, *13*, 284.

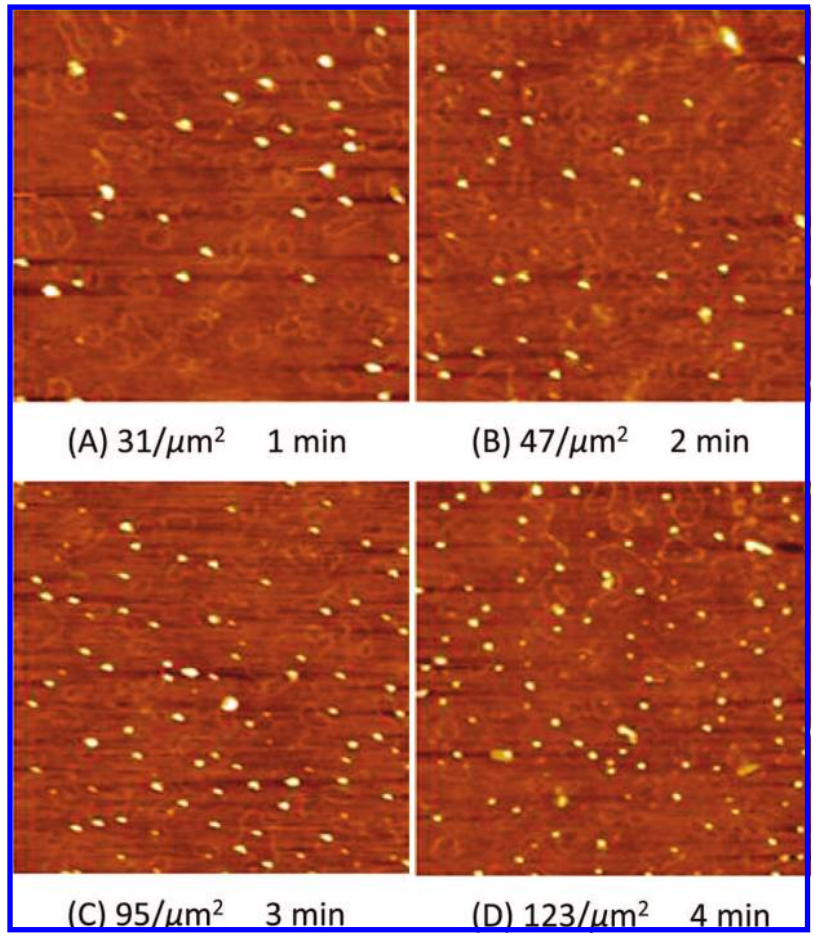


**Figure 2.** Representative AFM micrographs, measured dry, of cationic nanoparticles on acid-etched microscope slides. Each image is 1 × 1 $\mu$m$^2$.

particle adhesion: there is no evidence for diffusion of the nanoparticles on the surface during the deposition or drying process. Indeed, the particles exhibit no removal on drying, immersion in organic solvent, or sonication in aqueous or organic solvent. Whereas the initial driving force for particle deposition is the electrostatic attraction between the cationic groups on the nanoparticles and the negative silanols on the silica flat, strong van der Waals forces likely hold the particles in place.

For the range of collecting surfaces used in microparticle capture experiments in this study, up to 150 nanoparticles/$\mu$m$^2$, the collecting surfaces themselves were net negative, having $\zeta$-potentials within a few percent of that for bare silica, −58 mV at pH 6.1 in 0.005 M buffer. This was determined by examining the electrophoretic mobilities of 1 $\mu$m silica particles onto which known amounts of cationic nanoparticles had adsorbed, similar to our prior protocol.[43]

Studies of microparticle capture and resistance to shear forces were conducted in a flow chamber of similar design to that for nanoparticle deposition, except now with a clear back panel to facilitate illumination from the rear. This chamber was placed on a home-built lateral microscope where a 20× objective focused the image of the collecting surface onto a video camera. A suspension of monodisperse 1 $\mu$m silica particles (1000 ppm) from Geltech (Orlando) in pH 6.1 phosphate buffer, with an ionic strength of 0.005 M, flowed at a wall shear rate of 21 s$^{-1}$ over each nanoparticle-containing silica flat. (The flow chamber was oriented vertically so that gravity did not affect particle adhesion.) The silica particle capture rates represent steady-state particle capture, typically established within ∼1 min of microparticle flow. The rates were measured well before surface crowding of the silica microparticles hindered the capture of additional microparticles. Thus, the data are representative of many microparticle−collector interactions.

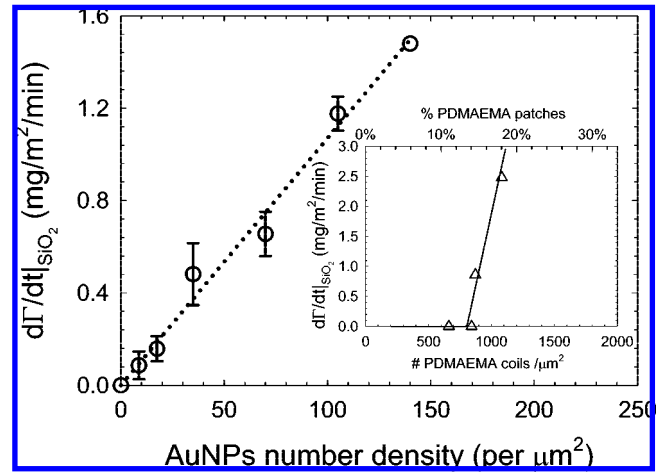


**Figure 3.** Capture Rates of 1 $\mu$m spherical silica particles, d$\Gamma$/d$t$(SiO$_2$) from flowing suspensions in pH 6.1 buffer, 0.005M, $\kappa^{-1}$ = 4.24 nm. The inset contains data from ref 26.

## Results

The dynamic capture of silica microparticles on a series of surfaces containing different densities of cationic nanoparticles is shown in Figure 3. Here the microparticle capture rate on these surfaces increases linearly with nanoparticle density on the substrate, starting at the origin. This seemingly straightforward

(43) Shin, Y. W.; Roberts, J. E.; Santore, M. M. *J. Colloid Interface Sci.* **2002**, *247*, 220–230.

result represents an extreme in the behavior of microparticle capture. The observation that the data approach the origin suggests that no matter how sparsely the cationic nanoparticles are positioned on the surface some silica microparticles will eventually be captured. Without any nanoparticles, however, the collecting surface captures no silica microparticles. This means that a silica flat containing only one cationic nanoparticle would eventually capture and hold a silica microparticle. Thus, these cationic gold nanoparticles, when placed on a negative surface, are each capable of capturing and holding a much larger object.

The significance of the intersection with the origin in Figure 3 is put into perspective by a comparison to the ability of a second type of surface to capture the same 1 $\mu$m silica particles. We previously reported[26,27] on collecting surfaces that contained 11 nm cationic polymer "patches" that held their positive charge relatively flat to the surface compared with the raised nanoparticles in the current study. With the flat cationic patches, the rates of 1 $\mu$m silica particle capture (at the same pH and ionic strength as in Figure 3) showed a positive $x$ intercept near 800 patches/$\mu$m$^2$ rather than passing through the origin. Therefore, the collecting surfaces decorated sparsely with cationic patches were completely nonadhesive toward approaching negative microparticles. This behavior suggested that the mechanism of microparticle capture involved multiple cationic patches acting on a single silica microsphere. As pointed out by a reviewer, the new data employing nanoparticle-functionalized surfaces happen to employ a wall shear rate of 20 s$^{-1}$ whereas the older data in the inset with the cationic patches were at a flow rate of 39 s$^{-1}$. This difference was a result of the different flow cells on the different instruments in the two studies. We previously reported that, with the cationic patches, there is a wall shear rate to the $^1/_3$ power of the microparticle capture rate.[28] For this reason, the factor of 2 difference between 20 and 39 s$^{-1}$ is actually quite small. We have obtained additional data with the nanoparticle-functionalized surfaces that show for wall shear rates of at least up to 100 s$^{-1}$ data such as those in Figure 3 continue to pass through the origin. Therefore, the qualitative differences between particle capture by surfaces functionalized with flat patches and those functionalized with cationic nanoparticles is preserved over a wide variety of flow rates.

The action of the flat cationic patches mimics the common biological situation where multiple ligand−receptor bonds engage at cell−cell contacts, whereas the current data in Figure 3 represent the more extreme behavior. By comparing the current data with this prior work, we conclude that the difference between the need for multiple interactions versus a single contact to capture a microparticle results from the raised nature of the current cationic nanoparticles. Whereas it is generally understood that placing adhesive elements away from a surface increases their impact (for instance, placing antibodies on polymer tethers), this work quantitatively demonstrates how the relative range of attractive and repulsive interactions translates to dynamic adhesion and particle capture.

To reinforce the similarities between the current nanoparticle-based cationic moieties and the flat cationic patches, it should be noted that both are 11 nm in diameter and contain 200 positively charged groups. In the adsorbed polymer (flat patch) case, all positive charges are potentially exposed to the solution, but the actual charge after counterion condensation is about 75. In the case of the current nanoparticles, the positive charges are spaced over the surface of the sphere so that counterion condensation is much smaller; however, roughly half of the cationic charge lies between the nanoparticle and the substrate so that approaching silica microparticles do not feel the attraction from roughly half,

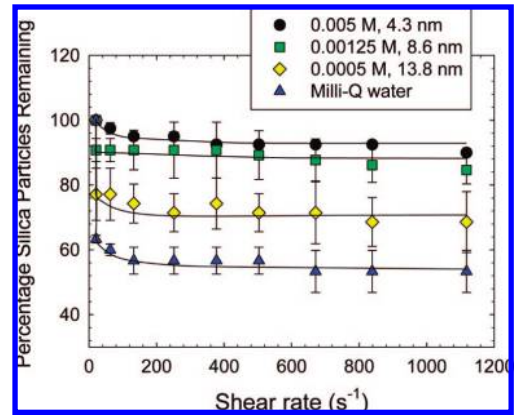


**Figure 4.** Fraction of silica particles remaining after the ionic strength and shear rate have been adjusted to remove adherent silica particles. The silica particles were deposited in 0.005 M pH 6.1 phosphate buffer onto a collecting surface with 9 cationic nanoparticles/$\mu$m$^2$. All data points are relative to this initial condition for silica adhesion. Curves guide the eye and emphasize that all data sets start with 100%.

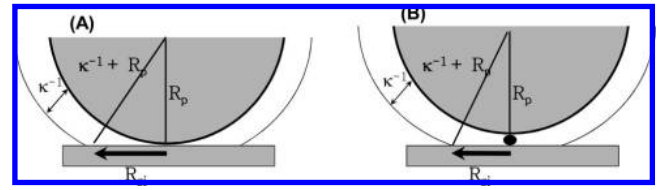


**Figure 5.** (A) Limited collector, over an area of radius $R_{zi}$ (zone of influence) acting a particle, depending on the Debye length. $R_{zi}$ can be smaller, when aparticle rests on a single nanoparticle, making an encounter with a second nanoparticle less influential.

about 100, of the cationic groups. The primary difference, then, between the collecting surfaces is that with the nanoparticles some of the positive charge is placed beyond the electrostatically repulsive surface field of the silica.

Another interesting point of comparison between the nanoparticle-bearing surfaces of Figures 3 and other adhesive situations involving 1 $\mu$m spheres is that the contact area between the microsphere and nanoparticle-containing surfaces, which is on the order of 80 nm$^2$, follows from the diameter of the nanoparticle squared. The same microparticle interacting with an electrostatically attractive flat substrate at this ionic strength will have an effective contact area of 13 000 nm$^2$ based on the intersection of the Debye layer around the sphere (4.24 nm in the case of the 0.005 M buffer) with a planar surface. Hence, in the case of the current study, the contact between the microsphere and the collector is localized by the nanoparticles, and this in turn constitutes a means of applying force to an extremely small region of contact.

The forces that capture the silica particles in Figure 3 turn out to be quite strong and hold the silica particles on the otherwise repulsive silica flat under strong shear. Figure 4 illustrates this point by examining the behavior of 1 $\mu$m silica particles that have already adhered to collecting surfaces and are subsequently challenged by strong shear or different ionic conditions. In Figure 4, the collecting surfaces contain 9 nanoparticles/$\mu$m$^2$, which is in the regime where silica particles are held by single nanoparticles to the collector. (This condition corresponds to the sparsest nanoparticle datum in Figure 3.) The argument for action by single nanoparticles follows from the limited area on the collecting surface that is actually able to interact with a micrometer-sized sphere, in Figure 5. The 4.24 nm Debye-length shell around a 1-$\mu$m-diameter sphere intersects a planar surface, subtending a

radius of 65 nm. Therefore, only 13 377 $nm^2$ (0.013 $\mu m^2$) of the collecting surface exerts an electrostatic force on a micrometer-sized silica sphere in contact with the surface. Assuming a random (Poisson) distribution of nanoparticles on the collecting surface with an average of 9 nanoparticles/$\mu m^2$, the probability ratio of encountering one versus two nanoparticles over an area of 13 377 $nm^2$ is 16.6. Hence, there will be more than an order of magnitude more silica particles held by one rather than two nanoparticles. This represents a worst case estimate because electrostatic repulsions between nanoparticles during the deposition process likely truncate the Poisson distribution of gold nanoparticles. That is, AFM data in Figure 2 and other similar images reveal negligible occurrences of closely situated nanoparticle pairs on collecting surfaces.

In generating Figure 4, we first allowed approximately 30 silica particles to be captured from a gentle flow (a wall shear rate of 21 $s^{-1}$) and an ionic strength of 0.005 M (corresponding to a Debye length of $\kappa^{-1} = 4.24$ nm) in the field of view (128 $\mu m \times 96\ \mu m$) of the microscope. This avoids particle−particle interactions and related hydrodynamic effects. Studies were repeated with multiple slides, and different regions of each slide were examined. After the silica particles were allowed to adhere, the flow was increased stepwise, ultimately up to a wall shear rate of 1118 $s^{-1}$, corresponding to a force of 9 pN on an immobilized nanoparticle.[44,45] The experiments were repeated with fresh slides, always depositing the gold nanoparticles from DI water and adhering the silica microspheres at an ionic strength of 0.005 M and a shear rate of 21 $s^{-1}$ but then subsequently adjusting the ionic strength to a new level (to generate an entirely new family of data) and subsequently increasing the flow rate after that. We observed that particles were released mostly when the ionic strength was reduced, rather than when the shear was increased. This indicates that though the interactions are strong (from the practical perspective) they are also reversible.

As shown in Figure 4, shear had little impact on silica particle retention at several ionic strengths. For each ionic strength, roughly 5−10% of the particles were removed as the shear was increased from 21 to 133 $s^{-1}$. Further increases in shear, up to 1118 $s^{-1}$, did not substantially dislodge particles. The ionic strength was, however, more important than shear, which is a result of the predominantly electrostatic nature of the interactions. Figure 4 indicates that increases in the Debye length above 9 nm caused a substantial fraction of the particles to be released under gentle shear conditions. Debye lengths of less than 9 nm had only a small effect on silica particle retention. This is consistent with the 11 nm particle size.

The insensitivity of particle retention to shear demonstrates that the electrostatic forces are orders of magnitude stronger than the hydrodynamic forces. Furthermore, the sensitivity of particle retention to ionic strength demonstrates the importance of electrostatics relative to van der Waals attractions. As the Debye length is increased, so too follows the range of the electrostatic attractions from the nanoparticles and the electrostatic repulsions from the underlying substrate. As the Debye length approaches the particle diameter, the fact that the nanoparticle attractions protrude from the background repulsive field becomes unimportant: with a greater area of repulsive chemistry relative to a small single nanoparticle, repulsions dominate at large Debye lengths, causing silica microparticles to be released. There are, of course, practical experimental limits on the Debye length, for instance, from dissolved gases. Also, as one moves in the direction of large Debye lengths, the buffering capacity of the solution is lost, hence the silica surface potential is not controlled and silica repulsions become compromised. We have confidence, therefore, in the 13.8 nm Debye length in 0.0005 M buffer (based on pH and conductivity) and observe that the Debye length in fresh DI water is greater, but we cannot quantify the latter.

## Summary and Perspective

We have demonstrated how negative surfaces presenting cationic nanoparticles capture and hold silica microparticles flowing in solution at controlled pH and ionic strength. Without the nanoparticles, the silica surfaces repel the 1 $\mu$m silica spheres; however, the cationic nanoparticles produce localized attractions that trap flowing micrometer-scale particles. The rate of microparticle capture increases linearly with the surface density of cationic nanoparticles, starting at the origin, indicating that each nanoparticle is capable of capturing and holding a microparticle. When the Debye length is smaller than the nanoparticle height on the surface, microparticles resist hydrodynamic shear forces exceeding 9 pN; however, as the Debye length is increased toward the nanoparticle size (and protrusion from the surface), the silica microparticles are released in a gentle flow. This represents a crossover from dominance by localized attractions at low ionic strength to control by the background electrostatic repulsive field. Thus, the electrostatic forces dominate hydrodynamic and van der Waals forces such that particles can be captured and released by changing ionic conditions. This behavior could form the basis for extremely sensitive detector elements. Also, because the localized nature of single nanoparticle−microparticle contacts differs from the many contacts that occur between most cells as part of signaling, using single nanoparticles may prove to be a useful means to manipulate cells and bacteria without triggering a biological response.

**Acknowledgment.** M.M.S. and J.M.D. acknowledge support from NSF-CBET-0428455. V.M.R. acknowledges support from NIH-GM-077173. Support from UMass MRSEC DMR-0213695 was also key to facilitating these studies.

LA800857V

(44) Goldman, A. J.; Cox, R. G.; Brenner, H. *Chem. Eng. Sci.* **1967**, *22*, 637–651.

(45) Goldman, A. J.; Cox, R. G.; Brenner, H. *Chem. Eng. Sci.* **1967**, *22*, 653–660.